University of South Dakota

USD RED

Spring 2020

Current and Future Applications of 3D Printing Using Custom-Made Materials

Bridger T. Irons
University of South Dakota

CURRENT AND FUTURE APPLICATIONS OF 3D PRINTING USING

CUSTOM-MADE MATERIALS

by

Bridger T. Irons

A Thesis Submitted in Partial Fulfillment
Of the Requirements for the
University Honors Program

_____

Department of Chemistry
The University of South Dakota
May 2020

The members of the Honors Thesis Committee appointed
to examine the thesis of Bridger T. Irons
find it satisfactory and recommend that it be accepted.

_____

Dr. Grigoriy Sereda
Professor of Chemistry
Director of the Committee

_____

Dr. Bernie Wone
Assistant Professor of Biology

_____

Dr. Victor Huber
Associate Professor of Basic Biomedical Sciences

ABSTRACT

Current and Future Applications of 3D Printing
Using Custom-Made Materials

Bridger T. Irons

Director: Grigoriy Sereda, Ph.D.

The use of 3D printers has increased exponentially from its inception in the 1980s. Recently, the ability to design and create detailed objects has drawn the attention of many who wish to capitalize on this highly customizable process. With much of the focus in this industry being placed on finding new printable materials, many are overlooking the possibility of modifying existing materials. The aim of our research was to modify the materials already being used by 3D printers to alter their properties and explore future possible applications. We examined the addition of graphene powder, carbon microfibers, and other nanoparticles to these materials. Graphene was chosen because of its versatility, which we hypothesized would improve the mechanical strength of existing silicone and plastic materials. The nanoparticles were added to the silicone to explore possibilities of drug delivery. Additional research was conducted regarding the current research and future applications of 3D printing and the associated technology.

KEYWORDS: 3D Printing, Graphene Powder, Carbon Microfibers, 3D Printing Applications

TABLE OF CONTENTS

LIST OF FIGURES

LIST OF TABLES

ACKNOWLEDGEMENTS

CHAPTER ONE

Introduction

The Early History of 3D Printing

Creative minds across the world possess the collective capacity to imagine objects that would revolutionize any industry. These inventions contain only theoretical value inside the minds of their prospective inventors. The true, tangible value of these conceptualizations can only be fully realized after said inventors produce a functional prototype of their imagined object. Though the steps an inventor takes to go from ideation to physical realization may seem simple, the process necessary to complete these steps requires a great deal of time. Many inventors find themselves struggling at the prototyping stage, as the creation of a single functional prototype is usually preceded by countless iterations of failed prototypes.

Manufacturing in the modern era often involves outsourcing the production of individual prototype parts to the appropriate producer. Skilled craftsmen then employ subtractive manufacturing techniques, which involves the breakdown of a large object where material is removed in order to fit the necessary design (Pîrjan & Petrosanu, 2013; Kodama, 1981). While this outsourcing remains unavoidable for many manufacturers, it creates an obstacle in the form of time. Not only must you wait for a part request to be accepted, completed, and sent back, but if the part is not an exact fit, manufacturers may need to go through this process for multiple iterations of the part throughout the prototyping process.

Many have tried to address this particular time-consuming issue with prototype manufacturing. Ultimately, it is Hideo Kodama of the Nagoya Municipal Industrial Research Institute of Japan who is credited as having first demonstrated the next major prototype manufacturing revolution in 1981 (Rodriguez, 2014). He realized the time issue with invention and prototyping and attempted to reinvent how individual protype parts could be produced quickly, cheaply, and without requiring a great deal of labor. Kodama (1981) believed that instead of removing material to fit a design, computers and a specialized apparatus could utilize a new method of fabricating solid objects by way of "additive manufacturing" to enable prototyping and manufacturing at a much more rapid pace.

Hideo Kodama designed and built his own functional machine to accomplish his version of rapid prototyping (RP) additive manufacturing, which he would attempt to patent in 1981. This specific apparatus utilized a XY two-dimensional plotter that was hooked up to an ultraviolet (UV) light source using an optical fiber. Below the plotter was a movable plate inside a receptacle that was filled with a liquid mixture of unsaturated polyester, a polymer cross linking agent, and a polymerization initiator. The plotter was programmed to follow a certain path emitting the UV light that is able to create singular layers of the programmed design. The UV light would also be directed to strike specific areas of the resin reservoir by a mask the reservoir of photo-hardening polymer resin below and cause the process of polymerization to take place, allowing the individual layers to solidify directly to the previous layers below (Kodama, 1981). Kodama (1981) found that "solid models of rather complex shapes can be fabricated by this technique…. shapes [that] cannot be cut even by computer-controlled lathe" (p.1773). His success with fabricating

solid objects using additive manufacturing technology in such a short time, with very little

material cost, and without the need of manual labor was very promising. After a patent

filing oversight on Kodama's behalf, he would fail to establish patent protected ownership

of his new rapid prototyping (RP) technology, and instead resulted in his work becoming

public (Wohlers & Gornet, 2016). His now publicly available and well documented

functional product and techniques drew a great deal of attention across the world. Hideo

Kodama would prove to be incredibly influential in the growing manufacturing field of 3D

printing. Figure 1 and Figure 2 display Hideo Kodama's product's schematics and his first

printed object, respectively.
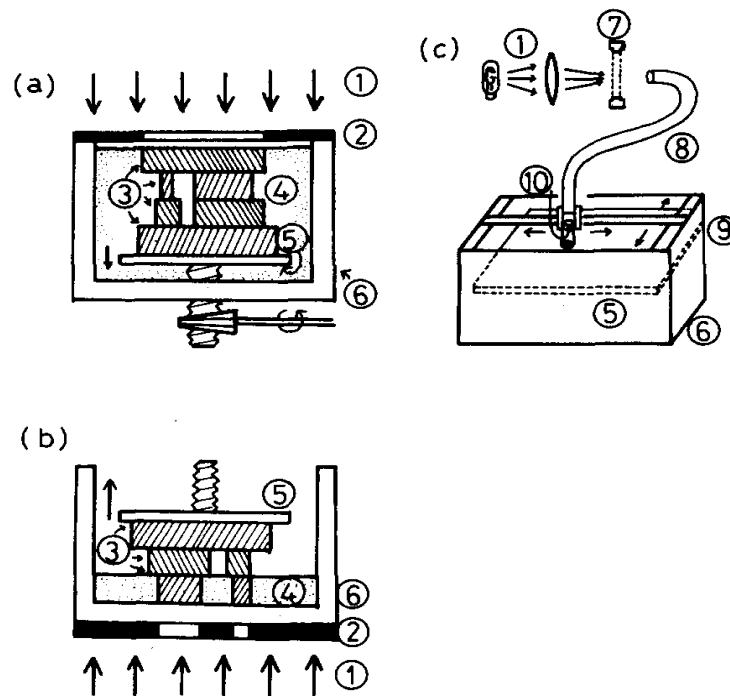
FIG. 1. Schematic sketches of three types of apparatus constructed in the present work. In this Fig. ① ultraviolet rays ② mask ③ solidified layers ④ liquid photo-hardening polymer ⑤ movable plate ⑥ receptacle ⑦ shutter ⑧ optical fiber ⑨ *XY* plotter and ⑩ optical lens. Exposure and shift of the movable plate is repeated in turn, and the solid model is grown on or under the plate.

Fig. 1: Hideo Kodama's schematic sketches and the original captions detailing his design components. From Kodama 1981.

3
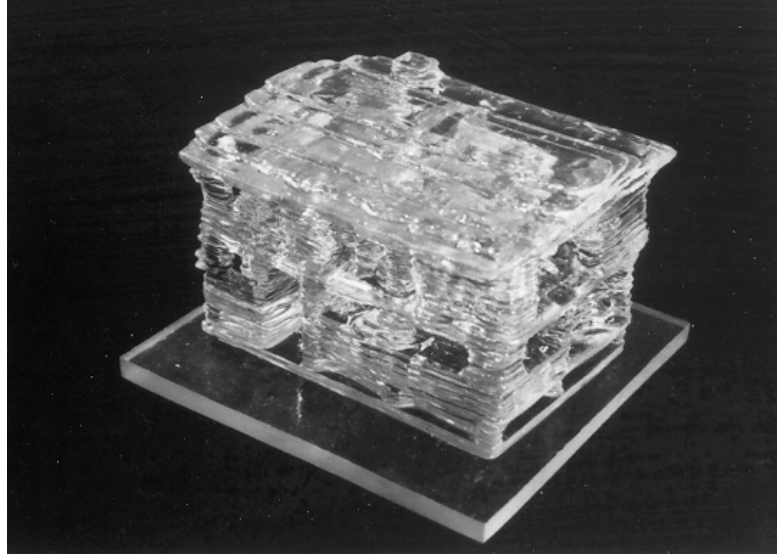
Fig. 2: First fabricated part using the Kodama experimental system. From Bourell et al. 2009.

Although Kodama's work was revolutionary, his failure to patent the design allowed others to incorporate his work into their own. This created a situation where the origin of 3D printing, as we know it, would actually be attributed to Charles Hull of the 3D Systems Corporation. Charles Hull was the first person to apply for a U.S. patent for his stereolithography apparatus and associated technology in the year 1984 and would ultimately be issued the patent in 1986, thus asserting Hull as the father of 3D printing (Wohlers & Gornet, 2016). The term stereolithography was coined by Hull to describe the implementation of additive manufacturing that was effectively a minor improvement to Hideo Kodama's rapid prototyping technology. The main difference between the two technologies was that Hull's version was capable of producing much more intricately designed parts with his machine's higher resolution than Kodama had ever documented (Wohlers & Gornet, 2016). The Stereolithography Apparatus 1 (SLA-1) would become the first commercially available additive manufacturing machine in 1987. This machine in

particular used a UV laser to cure its light-sensitive liquid polymer material, which contrasted with Kodama's UV optical fiber technique (Wohlers & Gornet, 2016). Following the commercial release of the SLA-1 by Charles Hull through his company, 3D Systems Corporation, the idea of 3D printing became an accessible reality for manufacturing companies and individuals across the globe. This introductory time frame for 3D printing would pave the way for further evolution of the industry as it expanded into fields and applications outside the scope of prototype manufacturing. Figure 3 contains a photograph of the SLA-1 and inventor Charles Hull being honored in 2016 for their contributions to mechanical engineering.

Fig. 3: Chuck Hull (right), current Chief Technology Officer and Co-Founder of 3D Systems receiving the American Society of Mechanical Engineers (ASME) Historic Mechanical Engineering Landmark from the former ASME President Bob Sims (left), in front of his SLA-1 3D printer at the ASME Historic Landmark Ceremony, which was held at 3D System' headquarters in Rock Hill, SC. From American Society of Mechanical Engineers, 2016.

Although there has been a great deal of growth in the 3D printing industry in the last 30 years, stereolithography, often abbreviated as SL or SLA, has remained a prominent 3D printing technology since it was first introduced. Outside interests would ultimately begin looking at both improvements and variations of this budding technology. The motivation of many who decided to embrace the technology was often rooted in the

potential applications of 3D printed products, which would drive innovation within the industry. Soon, many other versions of 3D printing technologies would emerge. As inventors and investors sought out and perfected more advanced methods using a wider variety of materials, interest in 3D printing would only continue to gain traction. Ceramics and metals were among the first group of materials that would become printable with new versions of 3D printing technology, joining the collective group of photo-curable polymers (Rodriguez, 2014). However, the dominant 3D printable material in terms of both cost and function, thermoplastics, would soon become the focus of the industry.

S. Scott Crump, founder of the prominent 3D printing company Stratasys, would be awarded a patent for his fused deposition modeling (FDM) technology in 1989, which was the most influential advancement in 3D printing since its introduction (Grant, 2005). Crump's technology, known more commonly today as either fused filament fabrication (FFF) or material extrusion, would introduce the use of thermoplastics as a viable 3D printing material. This style of extrusion-based 3D printing is typically what the general public associates with 3D printing. Material extrusion 3D printing is defined by the use of an electronically created three-dimensional model, which is then printed using an extrusion head or nozzle programmed to extrude material at a certain rate in progressive layers according to the model. Thermoplastics, which are production grade plastic polymers that are heated to temperatures near their melting point in order to allow these polymers to be extruded in a controlled manner, would become the material of choice for this style of printing (AMFG, 2020). Thermoplastics used in this version of printing usually come in a spool of filament, with the filament being composed of either polycarbonate (PC), polylactic acid (PLA), acrylonitrile butadiene styrene (ABS), nylon, acrylic, polyethylene,

or other high-performance materials (AMFG, 2020; Stratasys Direct Manufacturing, 2017). Figure 4 outlines the printing mechanism of fused filament fabrication.
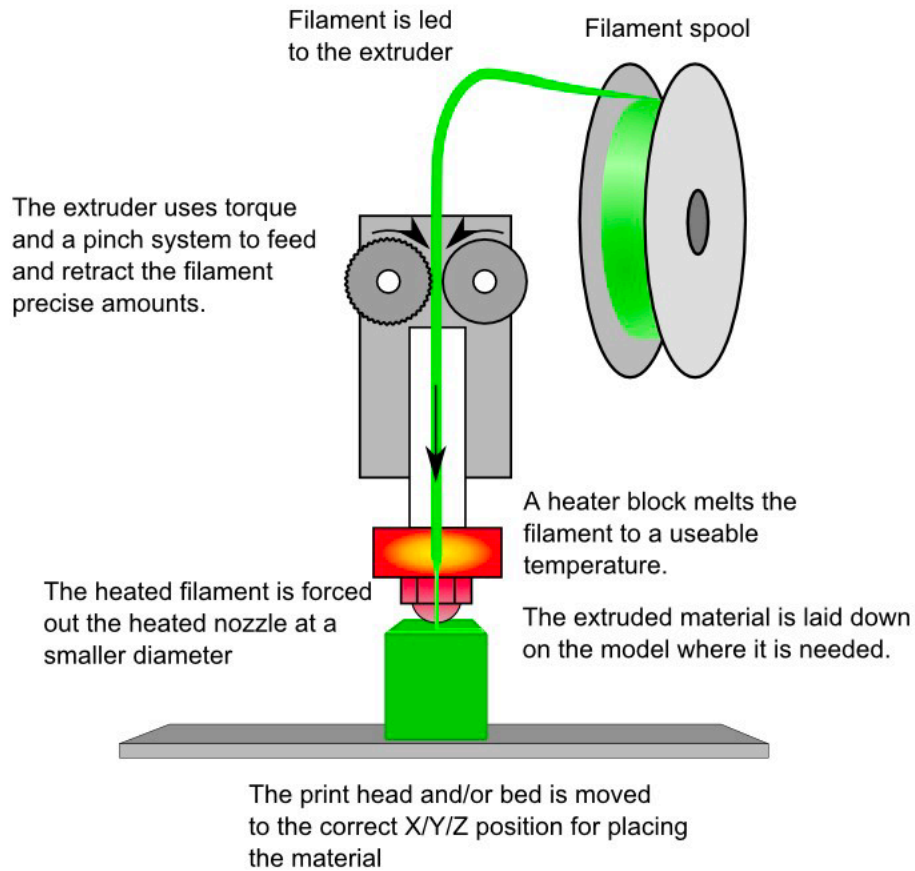
Fig. 4: Illustration of the mechanism behind a fused filament fabrication 3D printer. Displays how the material, in filament form, is fed into 3D printer, then extruded through the heated nozzle according to the designated design. As indicated, the printer will either have the print head or print bed move, depending on the specific make and model of the printer, in order to match the designated design. From 3D Printing for Beginners n.d.

S. Scott Crump's patent on his material extrusion FFF technology would expire in 2009 and result in a massive shift within the industry (Grant, 2005). 3D printers have

become increasingly affordable and easier to use as his original technology has been expanded and improved upon by other manufacturing entities. This large reduction in entry cost and necessary expertise associated with 3D printing, specifically material extrusion 3D printers, has greatly increased the accessibility of this technology. Currently, inventors, researchers, and enthusiasts alike are now able to purchase their own desktop sized 3D printers for just a fraction of the price when compared to less than a decade ago. With newfound freedom due to increased availability in both private and corporate manufacturing, the work to expand the capabilities and applications for 3D printing have exponentially increased. Many in the industry are focusing on finding new printable materials, thus largely overlooking the possibility of modifying materials that are already capable of being used by any current 3D printer.

Identifying an Opportunity

The aforementioned oversight was what motivated Dr. Sereda and I to apply for the University of Nebraska-Lincoln's Nebraska Nanoscale Facility (NNF) Professor/Student Pair Summer Research Fellowship. The NNF is a member of the National Nanotechnology Coordinated Infrastructure (NNCI), which is comprised of 16 major nanomaterial research centers in the United States and is supported by the National Science Foundation (NSF) and the Nebraska Research Initiative. With this grant, we had the opportunity to spend the summer of 2018 at the NNF on the University of Nebraska-Lincoln campus. During our time here, we would have access to multiple cutting-edge 3D printers and their respective technologies, and to lab personnel who could ensure proper operation of said machines.

The initial goal of our project was to develop a technology capable of 3D printing biocompatible and mechanically strong implant components from a customized

thermoplastic or silicon material. We believed that we would be able to significantly alter the mechanical properties of components created via 3D printing by adding pristine, sized, and functionalized carbon microfibers, as well as functionalized graphene, to 3D printer compatible polymer filaments. These carbon nanomaterials would be prepared beforehand at the University of South Dakota (USD) by Dr. Sereda's graduate student, Ramon Sarder, according to our patented technology (U.S. Patent No. 10316010, 2015). Once the appropriate carbon nanomaterials were produced by Sarder, we would use X-ray photoelectron spectroscopy (XPS) technology at the NNF to analyze the functionalized carbon microfibers and functionalized graphene powders prior to any further experimentation. Figure 5 shows one example of such carbon microfibers we hoped to use to modify existing 3D printer materials.
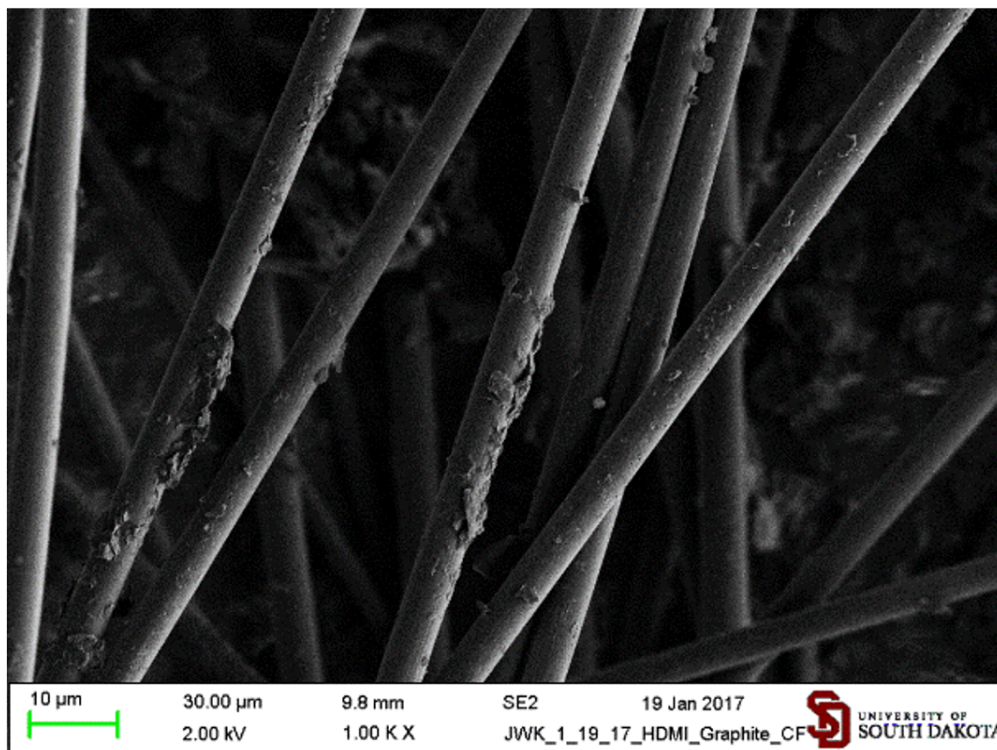
Fig. 5: Image of carbon microfibers modified by N-hexadecylmaleimide (HDMI) graphene, taken by a scanning electron microscope (SEM) at USD.

After a completed analysis, we intended to experiment with methods of incorporating both carbon fibers and graphene powders into existing 3D printable materials used by the various 3D printers at the NNF. The properties of the resulting modified 3D printable materials would then be examined using nanoindentation and environmental scanning electron microscopy (ESEM) technology. We then intended to take our modified materials and experiment with various printers in order to discover one capable of printing specific components of our choosing. In order to accomplish these tasks, I needed to explore the process of 3D printing an existing object. This included gaining a sufficient competency using 3D scanning technology and 3D modeling software, allowing me to replicate objects. I also needed to learn how to use a filament extruder to properly make a carbon modified thermoplastic material capable of being used by a fused filament fabrication printer using the process outlined previously in Figure 4.

Pertinent Research Using the Nanoparticles of Interest

The inclusion of graphene into orthopedic devices has been a focus of research recently for improving the general cleanliness of such devices, as well as other uses. Recent work using reduced graphene oxide has shown that the incorporation of this form of graphene into wound coverings may be beneficial for patients with poor vascularization and slow wound healing rates like those common among patients with diabetes. Thangavel and his team of researchers have experimented with diabetic rats attempting to encourage wound healing through the use of bandages and nanocomposite scaffolds loaded with the reduced graphene oxide (Thangavel et al., 2018). The results of their study showed that the incorporation of the reduced graphene oxide led to faster wound healing rates and improved vascularization, while also making use of the antimicrobial property of graphene

to kill bacteria. Although the specific mechanism behind the improved healing and vascularization is unclear, it was shown that subjects that received the graphene nanocomposite scaffold treatment had "enhanced angiogenesis, collagen synthesis, and deposition in treated wounds" (Thangavel et al., 2018, p. 252) Furthermore, they detailed reason to believe that the scaffold treatment and the presence of reduced graphene oxide played a large role in the quickening of the healing by recruiting macrophages to enhance the rate of the early inflammatory steps of the healing process (Thangavel et al., 2018).

In other labs, similar drug delivery applications are under investigation using both graphene and calcium carbonate core hydroxyapatite nanoparticles closely resembling those utilized in our work. The ability of these compounds to function as a drug delivery method has been well documented in the research of applicable 3D nanoparticles (Mohd Abd Ghafar et al., 2017). In the time since our research ended, I have been able to dive deeper into this topic. The calcium carbonate/hydroxyapatite nanoparticles we used were incredibly similar to those being used by the Jiangsu Province Science and Technology Support Program of China. Researchers there are investigating the use of a polysaccharide hydrogel embedded with both calcium carbonate and hydroxyapatite nanoparticles as a method for sustained drug delivery and bone tissue regeneration efforts. Their work has paved the way for an injectable hydrogel solution that could be used as a direct delivery method for drugs near an existing bone. Their solution has shown potential to function as a gel bone scaffold that could interface with existing tissue and help regenerate damaged bone and rectify irregular bone defects (Ren et al., 2018). The nanoparticles used in their work are similar in size and shape to the core-shell calcium carbonate/hydroxyapatite nanoparticles we used and served as the bases for their gel scaffold (Ren et al., 2018).

CHAPTER TWO

Methods and Materials

XPS Analysis

The first step in the journey toward modifying existing 3D printable materials with our carbon nanomaterials was to characterize the composition of the nanomaterials we intended to use. In order to do so, we used XPS technology to analyze the elemental composition of various samples of modified carbon fibers. The carbon fiber used was of the SGL-APS subtype and was provided by the SGL Corporation to Ramon Sarder for preparation at USD. Once the XPS analysis was completed, both Dr. Sereda and I began learning how to operate various 3D printers and their associated software. Table 1 shows the results of the XPS analysis. Figure 6 and Figure 7 display the 2D chemical structure of the two primary compounds used to modify the carbon fibers.

XPS Results	C (%)	N (%)	O (%)
Pyrolyzed SGL-APS carbon fibers	86.08	3.84	10.08
Pyrolyzed SGL-APS carbon fibers modified with 1,6-bismaleimidohexane	76.81	6.83	16.36
Pyrolyzed SGL APS carbon fibers modified with HDMI	89.61	3.81	6.58
Pyrolyzed SGL-APS carbon fibers modified with 1,6-bismaleimidohexane graphene	85.81	4.92	9.27

Table 1: Results of XPS elemental composition analysis of various modified and unmodified carbon fibers. Fibers prepared at USD by graduate student Ramon Sarder prior to analysis.

Fig. 6: (Left) 2D structure of 1,6-bismaleimidohexane, which was used to modify the second sample of carbon fiber, and to modify the graphene that was then used to modify the fourth sample of carbon fiber. From PubChem 2020a.

Fig. 7: (Right) 2D structure of N-hexadecylmaleimide (HDMI), which was used to modify the third sample of carbon fiber. From PubChem 2020b.

Exploration of 3D Scanning Technology

Before we could attempt to modify materials, I first needed to learn how to scan objects in the real world so they could be replicated using 3D printing technology. I focused on experimenting and gaining competency using the NextEngine 3D Laser Scanner. This scanner came with a tilting table that could be used to secure an object and use the motion of the table on all three-dimensional axes to obtain a near 360° 3D scan of an object. This scan was then converted using the NextEngine software to create an STL file. These STL files are 3D models that 3D printers use as blueprints for printing an object. STL files can also be created from scratch instead of a collection of scans. For our specific research, we wanted to examine the possibilities of printing a toe spacer using the 3D-

Bioplotter. I created an STL file for a toe spacer using the NextEngine Scanner and attempted to scan a retainer in order to test the resolution of the scanning technology and explore the possibilities of 3D printing a retainer or other denture components. Figure 8 and Figure 9 display the toe spacer STL model and the retainer in the settings window used to initiate the scan, respectively.
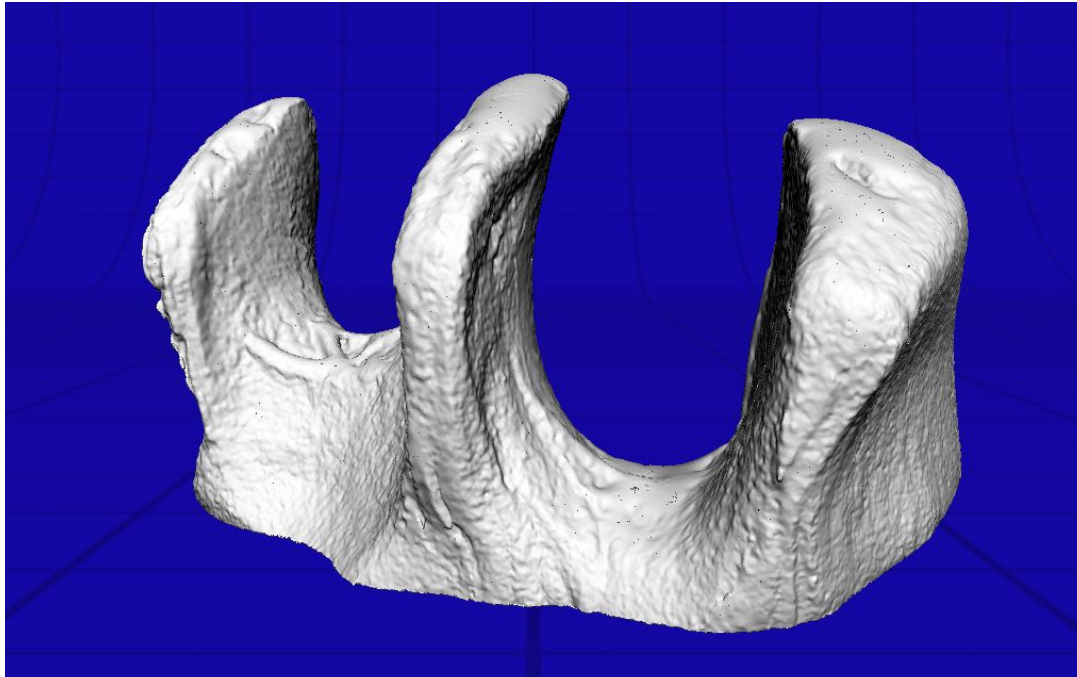
Fig. 8: Display showing the STL file of the toe spacer after being scanned by the NextEngine 3D Laser Scanner.
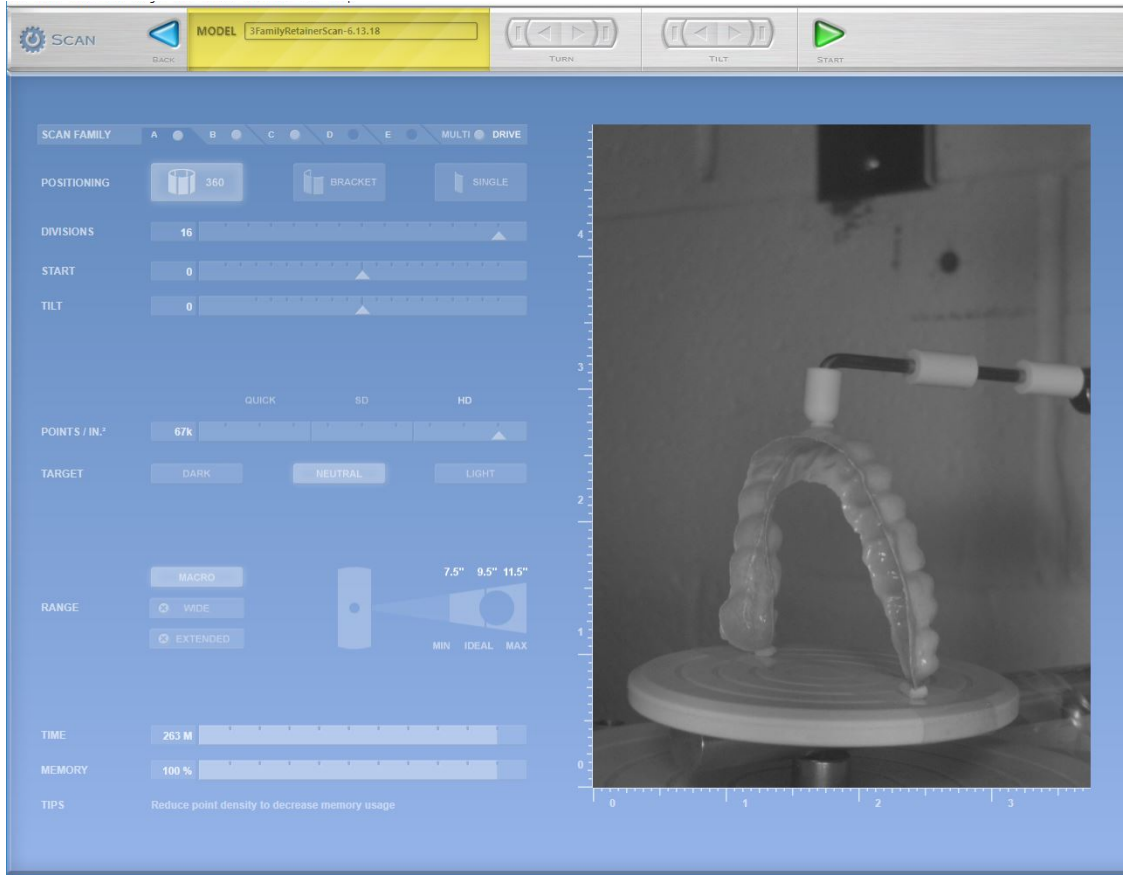
Fig. 9: Display of the NextEngine 3D Laser Scanner software prior to initiating a scan of the retainer, which was used to test the resolution of the scanner.

3D-Bioplotter

We began our search for 3D printers and materials that would be ideal for our experimentation purposes by first assessing the 3D printers available on the University of Nebraska Lincoln's campus in any department. Of those available, we settled on two particular printers. The first was the EnvisionTEC 3D-Bioplotter and its resin based in silicone. The second was the Hyrel 30M with the capability of printing with various thermoplastics, which will be discussed later on. Once we were properly trained on the basics of the 3D-Bioplotter, we began experimenting with the default silicone resin supplied by the manufacturer. This resin was placed into a pressurized syringe tube that

would be connected to the cold temperature extrusion head where it could be extruded under a variety of settings to match the material's viscosity and pourability to the intended job. For all prints we did, the base silicone resin refers to LT Demo Material 0.4, which was loaded into the Low Temp ID 1 extrusion tool, with a material temperature set point for the head of 23 °C. Every print done on the 3D-Bioplotter was performed onto the platform with the resin being printed onto a thin sheet of Low Temp Substrate that comes with the machine, at a platform temperature set point of 20 °C Figure 10 shows the EnvisionTEC 3D-Bioplotter we used.
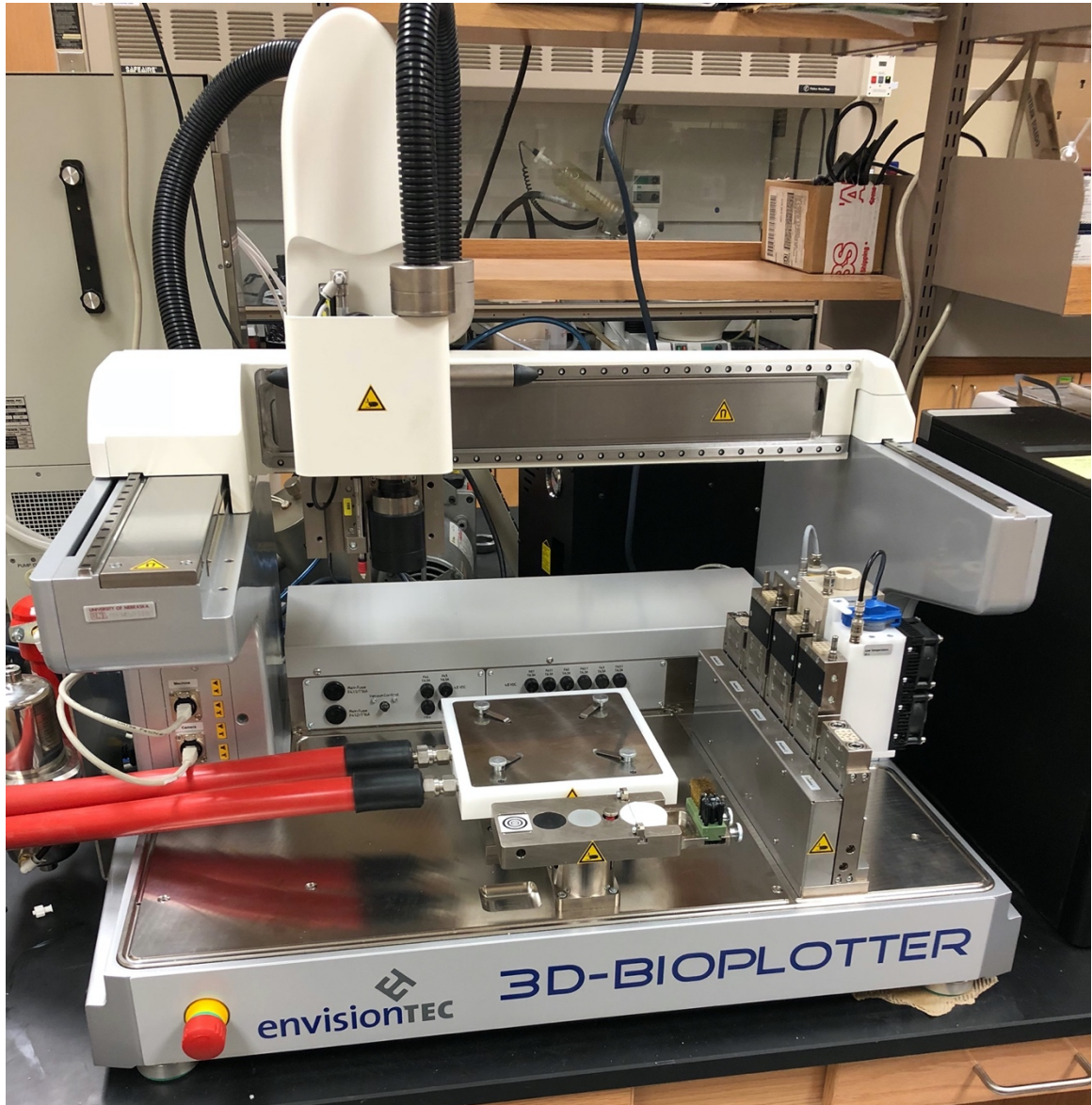
Fig. 10: Photograph of the EnvisionTEC 3D-Bioplotter we used to carry out our silicone-based resin prints. On the right side are the multiple heads the 3D-Bioplotter is equipped to use. The cold temperature extrusion head we used is in the opaque compartment, which holds syringes that are placed under and secured by the blue colored top. This is where the resin was held prior to printing and was where we would mix in our graphene and carbon fibers in prior to printing attempts.

After our training was complete, we made a couple prints to get comfortable with operating the machinery, then began experimenting with the base LT Demo Material. This printer in particular had a lot of settings and allowed for the customization of the inner structure pattern. The first thing we attempted to print was a toe spacer, which ended up being a somewhat failed attempt at a full print, as the machine's settings for our purposes were not yet perfected. Specifically, our problem was the inner structure pattern, which is the pattern the layers of print are filled in with after the outline of a layer is made. We initially used the "0.6 mm – 0 – 45 – 90 – 135 degrees" premade pattern. This pattern had the distance from the contour (outside border) as .3 mm and the distance between the center of the strands was 0.6 mm. The strand extruded from the Low Temp head was 0.4 mm in diameter. The result was a 77-layer product that had an inner pattern that was too spaced out, therefore appeared porous and was much flimsier than we intended.

Our second attempt utilized a different inner structure pattern titled "0.3 mm – 45 – 135 degrees". In addition to changing the inner structure fill pattern, we also used the Low Temp head to extrude a strand that was .3 mm in diameter, and would be 0.15 mm from the contour, and had a distance of 0.30 mm between individual strands within a layer. This resulted in a print that looked like a cohesive structure that was less flimsy when compared to the porous toe spacer and looked much more like the scanned toe spacer these were meant to represent. Table 2 outlines the specific settings chosen on the 3D-Bioplotter interface that remained consistent when completing both the toe spacer prints and the pad prints to be discussed in the following paragraphs. Figure 11 shows the porous toe spacer mid print allowing the chosen inner structure pattern to be viewed.

Build Parameter	Chosen Setting
Platform Height Control	On
Clean Needle before Start	On
Transfer Height	5.0 mm
Needle Offset	0.40 mm
Layer Height	0.320 mm above previous layer
Build Inner Structure	On
Build Contour	On
Random Start Position	On
Low Temperature Material	LT Demo Material 0.4

Table 2: Build parameter and settings for printing the toe spacer using the original scan from the NextEngine 3D Laser Scanner as the STL file blueprint and for the custom-made silicone and graphene pads detailed in the following paragraphs. Any settings that did not apply or were not used within the Project Editor screen of the software are not included.
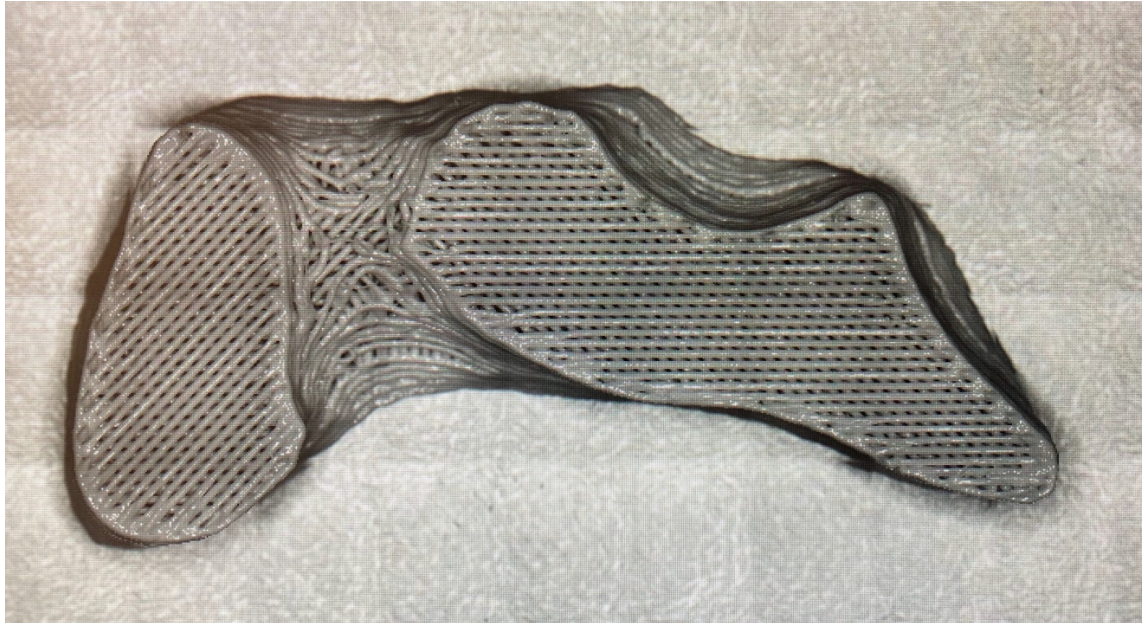
Fig. 11: Image taken by the 3D-Bioplotter's attached camera during the middle of the toe spacer print. The chosen inner structure pattern was the 0.6 mm – 0 – 45 – 90 – 135 degrees, which indicates that the print nozzle was placed 0.6 mm from the midline of the adjacent extruded line of silicone resin, and that the pattern of parallel lines each layer is comprised of was rotated by 45° clockwise for each successive layer. In this image it is evident that it was captured mid print and mid layer, where the left portion of the print is one layer ahead of the right portion.

Once the toe spacer print was completed, we began experimenting with different ways to incorporate our carbon materials into the silicone resin we now had experience using. First, I attempted to add a small weight percent (<3%) of the pyrolyzed SGL-APS carbon fibers to the silicone resin using manual homogenization but was unable to disperse the fibers from one another enough to be successful. The result was a mixture that was relatively homogenized but contained carbon fibers that were simply too large to be

effectively extruded through the head in a continuous manner. Attempts were made to alter the pressurization and extrusion rate of the cold temperature print head without any success.

Our next option was to use the 1,6-bismaleimidohexane functionalized graphene. This carbon nanomaterial was also produced at the USD campus by Sarder. Our hope was that this finely powdered 1,6-bismaleimidohexane functionalized graphene would be able to be homogenized effectively with the silicone resin. We started with a small weight percent of graphene (0.24%) and successfully homogenized the resulting custom-made material inside the 3D-Bioplotter extrusion tube. The choice was made to use the design of a 10 mm x 10 mm x 10 mm box. Our actual print was not 10 mm in height, as we ended up actually a 10 mm x 10 mm x 1.28 mm rectangle. The height was a result of 4 layers at 0.320 mm per layer, using the settings detailed above in Table 2. We referred to the resulting rectangle as a "pad". The inner structure pattern for all pads, unless otherwise stated, was the "0.25 mm – 45 – 135 degree" pattern that had a 0.25 mm diameter extruded strand of material that was 0.12 from the contour and had 0.25 mm between strands. We found success not only mixing our 1,6-bismaleimidohexane functionalize graphene into the silicone resin, but we had also been able to print an object that could be used for inspection via nanoindentation and SEM analysis.

Given the level of ease at which we were able to evenly distribute the graphene powder within the silicone resin, we decided to push the boundary. Our next attempt was to use a larger weight percent of graphene (3.8%), homogenize the newly custom-made material inside the same extrusion tube, then try and print an identical object. We were able to complete the same 10 mm x 10 mm x 1.28 mm rectangular pad. Next we tried

graphene into the silicone resin. After failing at incorporating and properly printing larger weight percentages (8% and 6.5%), we learned that the addition of 1,6-bismaleimidohexane functionalize graphene above a weight percent of 5% caused the printing process to become more difficult. The main problem seemed to be that the graphene, like the carbon fibers from our previous attempt, would stay together if in too high of a concentration and result in the pressurized head either becoming clogged, or sputtering out a discontinuous line of the custom resin. Thus, a weight percent of 5% 1,6-bismaleimidohexane functionalize graphene was the third pad to be made. The fourth pad was made using the default LT Demo Material silicone base.

Lastly, Dr. Sereda had core-shell calcium carbonate/hydroxyapatite porous nanoparticles that we wished to experiment with as well. These nanoparticles were added to the silicone base resin at a weight percent of 1.8%. The procedure for creating this was the same as the procedure used in the previous pads, as homogenizing the calcium carbonate/hydroxyapatite porous nanoparticles was much easier than initially anticipated. Once we had the 10 mm x 10 mm x 1.28 mm rectangle pad created using the 1.8% core-shell calcium carbonate/hydroxyapatite nanoparticle custom-made silicon material, we used what was learned from the porous toe spacer to create a porous version of this pad out of the 1.8% core-shell calcium carbonate/hydroxyapatite nanoparticle custom-made silicon material that would be easier to analyze on SEM. This was done because the calcium carbonate/hydroxyapatite nanoparticles were hypothesized to be capable of operating as a drug delivery vector given the nature of these nanoparticles to have other compounds attached through a variety of procedures. If we could prove that the nanoparticles were well spaced out, then the porous shape may provide opportunities for delivery.

Theoretically, a compound attached to the nanoparticles could be released over time and delivered through direct contact to a patient. Results from the nanoindentation and SEM analysis of all printed pads will be discussed in the results section. Figure 12 shows the calcium carbonate/hydroxyapatite nanoparticles using a SEM at the University of South Dakota prior to experimentation at any of the UNL campus's facilities.
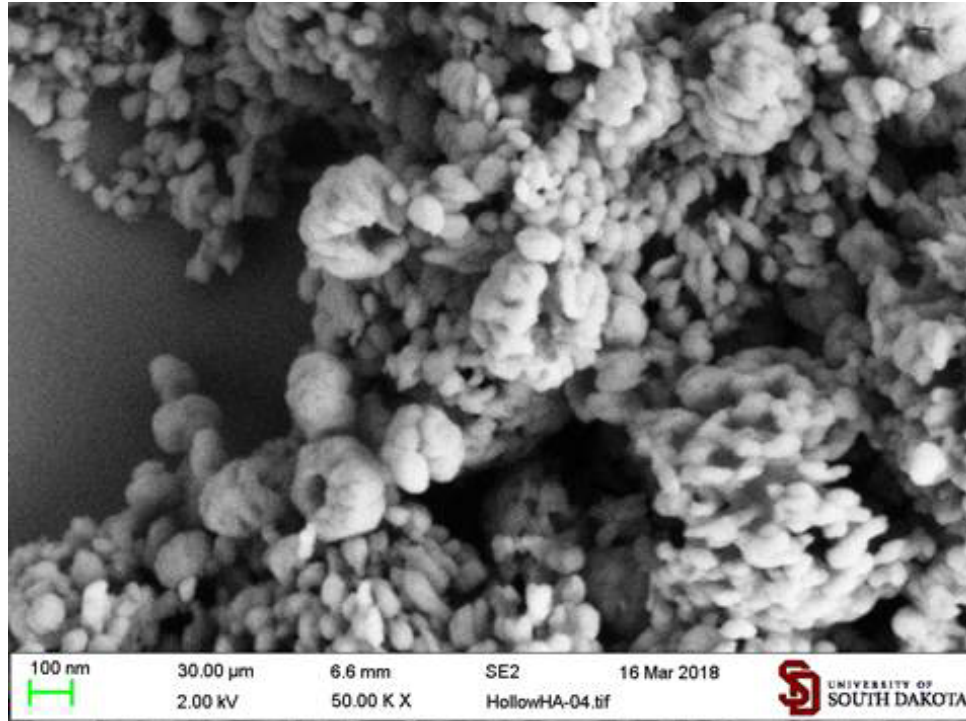
Fig. 12: SEM image of the core-shell calcium carbonate/hydroxyapatite nanoparticles taken at the University of South Dakota prior to our research at the University of Nebraska-Lincoln with the Nebraska Nanoscale Facility.

Carbon Modified Filament Production

As we went through possible applications of our carbon nanomaterials, both the fibers and the graphene, to produce custom-made materials for 3D printers, we knew we would be trying to augment some of the existing thermoplastic materials. In the world of 3D printing, thermoplastics have been a prominent fixture for some time now. Many in

the industry credit the continued use of thermoplastics to their ease of use and to their well-documented success being used to produce a wide variety of products. For this reason, we would be attempting to incorporate our carbon fibers and functionalized graphene into two types of filament used by FFF 3D printers. The two chosen thermoplastic filaments were acrylonitrile butadiene styrene (ABS) and polycarbonate (PC), which are widely used within the industry. These filaments are also compatible with the Hyrel System 30M FFF 3D printer, which we would be using for our experimental prints utilizing the carbon modified filaments we planned to produce.

In order to accomplish the goal of combining our carbon nanomaterials into these filaments, Dr. Sereda used grant funding to purchase a Filabot EX2 Filament Extruder. As a filament extruder, the purpose of this device is to take pellets of specific thermoplastics, which can be purchased in large quantities, and melt them down to then be extruded by the extrusion screw through one of the various interchangeable nozzles. If done properly, this allows the production of filament at a uniform thickness and density at a designated diameter, which can then be spooled together and input into a printer like the Hyrel System 30M FFF 3D printer we used. We placed an order for ABS pellets and PC pellets on the additive manufacturing company 3DXTech's website and upon receipt, I taught myself how to properly operate the Filabot EX2 using these pellets for both ABS and PC filaments. The 1.75 mm nozzle would be used for all filament production using the Filabot EX2.

The first filament produced using the Filabot EX2 was the ABS filament produced from ABS pellets. I placed the Filabot EX2 about 6 inches from the edge of a roughly 32-inch-high workbench to allow us to use the ground spool method and followed the general filament production procedure outlined in the manual. This indicated that the extrusion of

material starts with the operator filling the hopper, setting the temperature controller to the proper temperature for your material being used, which was 190 °C for ABS, and then placing the speed control dial set to a slow rate to start (< 0.25 max speed) while the "EXTRUDE" switch is still in the "OFF" position. Once loaded with the material, flip the "EXTRUDE" switch to the "ON" position and using the low speed control setting to allow the operator to ensure that the pellets have adequately melted together and are being consistently dispensed from the extrusion nozzle in the form of a continuous filament. When satisfied that the filament is coming out continuously and uniformly, the collection of usable material can be initiated. For the ABS filament production, I placed the speed control dial to approximately 0.67 max speed, guided the filament in straight line over the edge of the table so that it could be coiled on the ground for spooling and use in the Hyrel System 30M 3D printer.

With the ABS filament successfully printed, it was decided to make the modified ABS next. We measured out the amount of ABS pellets we would be using and then measured out an amount of 1,6-bismaleimidohexane functionalized graphene equaling a weight percent of 0.65%. These two components were then placed in a capped container to be shaken. The goal of the shaking was to have the thin powder of the graphene coat the outside of the pellets evenly. That way, when the pellets were heated and melted together to be extruded, the graphene would be as evenly distributed as possible. This hypothesis ended up being true, as the resulting modified ABS filament, produced using the exact same extrusion procedure as the regular ABS filament, appeared to have a uniform physical appearance and consistency.

In order to switch to the production of PC filament, we needed to purge the material still inside the machine. To accomplish this, we used the purge pellets that came with the Filabot EX2 and followed the purging procedure. For the purging, first remove the nozzle from the end and add roughly $\frac{1}{4}$ lb of the purge pellets into the hopper and run through the machine at the temperature used to produce the previous filament (190 °C for ABS). The purge pellets are white in color, so simply extrude the pellets until your extruded material returns to the white color of the purge pellets. Once the extrusion is white, place the pellets of the material you wish to extrude next into the hopper and run the machine at the new materials temperature. This meant adding PC and changing the temperature to 250 °C while watching for the extrusion to change color and match that of the pellets you added without any purge remnants. Continue extruding the material until it is run dry, turn off the extruder, and replace the extrusion nozzle. When this is done, you are now ready to extrude the next filament.

With the extruder ready for PC filament production, we followed the exact same procedure as the original ABS filament production. The only differences were that we had obviously added PC pellets instead, set the temperature for PC use at 250 °C, and placed the speed control dial to extrude at $\frac{1}{2}$ max speed. When this was completed, we followed the same mixing procedure to make PC modified with 1,6-bismaleimidohexane functionalized graphene at a weight percent of 0.64% initially. Once a 0.64% modified PC filament was produced, we then made another modified PC filament, this time containing 1,6-bismaleimidohexan functionalized graphene at a weight percent of 1.2%.

The production of these filaments was viewed as a success. The filaments that were modified with the 1,6-bismaleimidohexane functionalized graphene appeared to have a

relatively uniform consistency. Figure 13 shows the Filabot EX2 and the filaments produced using it.

Fig. 13: Image taken at the NNF facility showing the Filabot EX2 used for filament production, the ABS and PC pellet bags used during filament production, and (from left to right) filaments of ABS, ABS modified with 0.64% 1,6-bismaleimidohexane, and PC. The "dog bone" prints produced using each filament are also placed with their respective filament. These prints will be discussed below.

Printing with Modified Thermoplastics

With both modified and unmodified versions of both ABS and PC at our disposal, we began experimenting with the Hyrel System 30M. The Hyrel 30M is capable of utilizing many thermoplastics and is a comparatively cheap 3D printer when compared to other machines of similar capabilities. This printer operates using fused filament

fabrication printing method outlined previously in Figure 4. The culmination of our work using the Filabot EX2 to extrude materials would ultimately come down to whether our fabricated filaments, both modified and unmodified, were able to be printed.

The operator of this particular printer was Grant King, a graduate researcher attending the University of Nebraska-Lincoln. King was very familiar with the system and assisted us with loading our filament into the machine and setting up a print of an STL file that is typically referred to as a "dog bone". We were informed he would be using a dog bone print with a 45°-135° perpendicular crosshatching pattern that alternated angles each layer of print. The dog bone shape also lends itself to the testing of tension tolerances and other mechanical properties of the material used to 3D print the object. The print was done using the MK1-250 Standard Hot Flow modular head as the filament extruder, where the filament is heated to 230 °C prior to extrusion. When the filament is extruded, it is placed on a print bed that is heated to 90 °C. The print bed being heated surprised me, but King emphasized its importance explaining that a uniformly heated print bed maintains the proper adhesion of the first few printed layers to the bed. This is done until the print is finalized and can be uniformly cooled down. If the bed is not heated, the bottom layers of the printed design begins to cool off from the outside in, which leads to warping, where the outsides of the design curl up. Unfortunately, our time at UNL came to an end before we were able to print the PC modified with 1,6-bismaleimidohexane functionalized graphene at either the 0.64% weight percent or the 1.2% weight percent. Figure 14 shows the three dog bones we were able to print.

Fig. 14: Photograph of the 3D printed dog bones that are used to run tension tolerance tests and other mechanical tests to examine the properties of 3D printed thermoplastics. The dog bones (from left to right) are made out of acrylonitrile butadiene styrene (ABS) modified with 0.64% 1,6-bismaleimidohexane functionalized graphene, base acrylonitrile butadiene styrene (ABS), and polycarbonate (PC). All filaments used to print these materials were produced using pellets that had been heated and extruded by a Filabot EX2 in order to make printable filaments.

CHAPTER THREE

Results and Conclusions

Analysis of Graphene Modified Silicone Using Nanoindentation

Graphene has proven to be a remarkably versatile material with many advantageous characteristics that make it an ideal compound to incorporate into 3D printing. We hypothesized that the addition of graphene, specifically 1,6-bismaleimidohexane functionalized graphene, would imbue the resulting material with some of these properties. We wanted to see if graphene, which has recently been touted as one of the strongest materials ever measured, might contribute to an increase in hardness or strength of the resulting custom-made material (Lee et al., 2008). In order to test our hypothesis, we took the silicone pads we had created and tested the default silicone material pad against the pad made from the silicone modified with 1,6-bismaleimidohexane functionalized graphene at a weight percent of 5%. For comparison, we used a Hysitron TI 950 TriboIndenter to conduct nanoindentation hardness assessments on the two pads. Using this data, we were able to discern that the inclusion of a weight percent of 5% of 1,6-bismaleimidohexane functionalized graphene to the original silicone material used by the 3D-Bioplotter did not significantly affect the nanoscale mechanical properties of 3D-printed objects using the custom-made material. Table 3 shows the results of the hardness tests using the TriboIndenter.

TriboIndenter Data	Hardness (KPa)	Reduced Modulus (MPa)
Silicone pad	170 ± 6	2.52 ± .07
Silicone pad modified with 5% 1,6-bismaleimidohexane functionalized graphene	164 ± 13	2.46 ± .17

Table 3: Nanoindentation hardness measurements collected using a Hysitron TI 950 TriboIndenter. Data compares the unmodified and modified silicone pad prints made using the 3D-Bioplotter. Measurements were averaged out over 5 indentations per sample, with the ± representing the range of values.

**Analysis of Silicone Modified with Graphene and Calcium
Carbonate/Hydroxyapatite Nanoparticle Using SEM**

Next we analyzed the silicon modified and unmodified samples using scanning electron microscopy as we hypothesized the surface morphology would differ between samples. Images were taken of the pads made from the original silicone-based resin, the pad made from the silicone modified by a 5% weight percent of 1,6-bismaleimidohexane functionalized graphene powder, and the pad made from silicone modified by a 1.8% weight percent of core-shell calcium carbonate/hydroxyapatite porous nanoparticles. The calcium carbonate/hydroxyapatite nanoparticles were pictured earlier in Figure 12. Figure 15, Figure 16, Figure 17, and Figure 18 correspond to SEM images of the base silicone sample from a wider zoom, the base silicone sample from a closer zoom, the 5% graphene sample, and the 1.8% calcium carbonate/hydroxyapatite nanoparticles respectively.

HFW	mag	HV	spot	WD	pressure	humidity	⊢———— 500 µm ————⊣
1.75 mm	85 x	1.00 kV	3.0	7.7 mm	1.03e-3 Pa	---	UNL
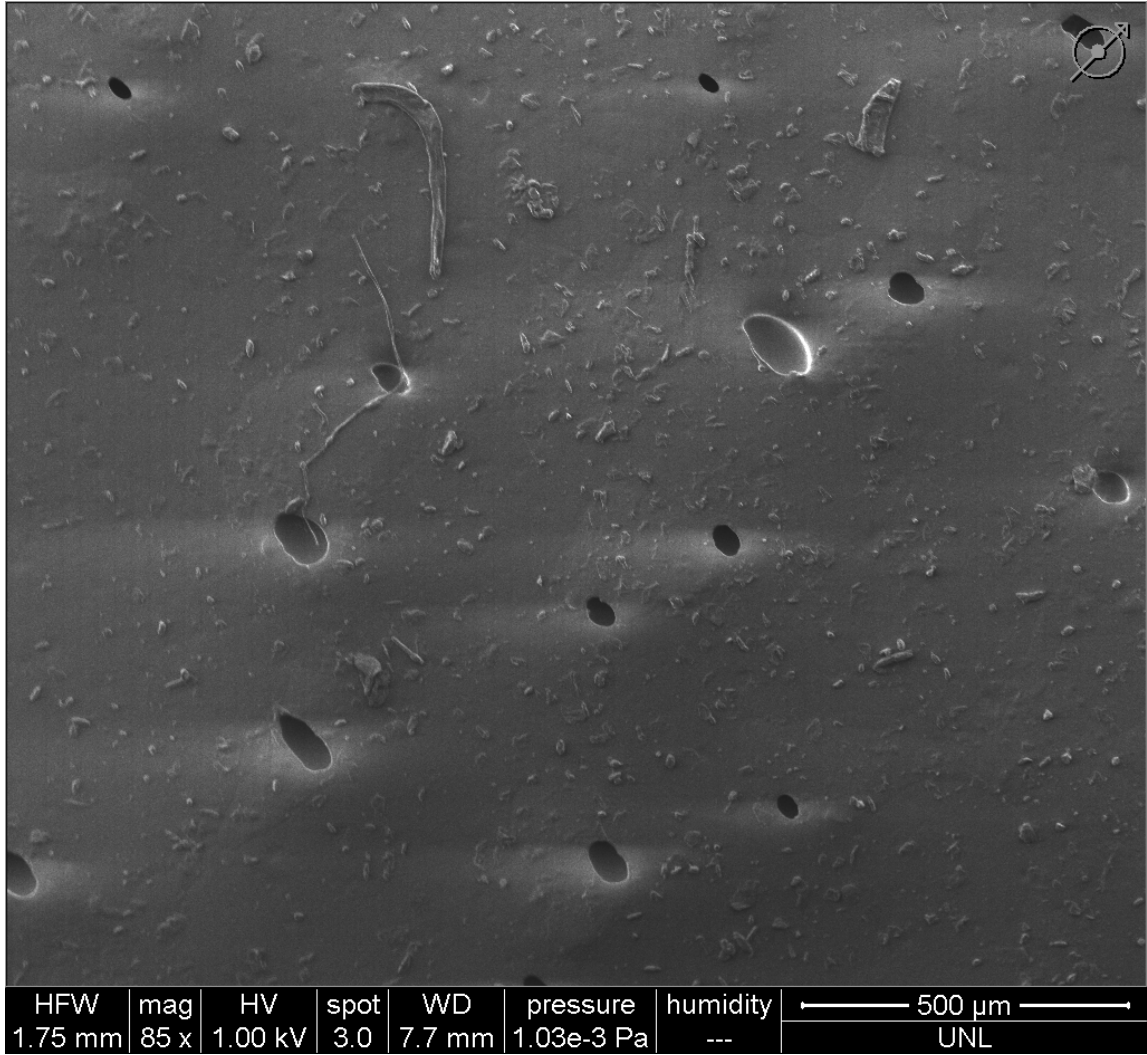
Fig. 15: SEM image of the pad printed using the unmodified silicone-based resin viewed at 85x magnification. Surface appears predominantly flat with small raised areas that are near 10-40 µm in diameter. Surface also has depressions that are less common and roughly 100 µm in diameter.
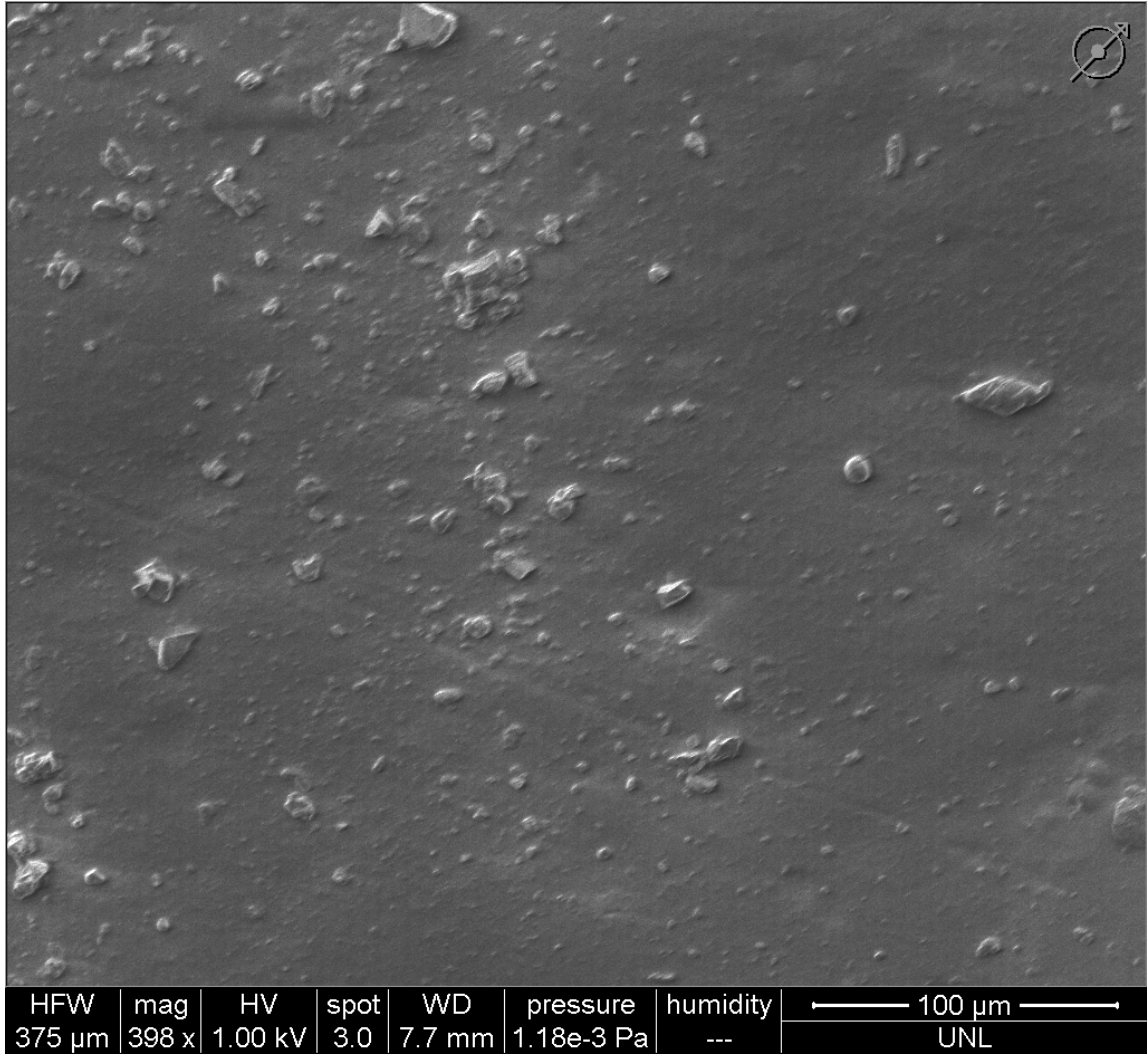
Fig. 16: SEM image of the pad printed using the unmodified silicone-based resin viewed at 398x magnification. Displays the raised surface areas, with diameters of 10-40 μm, that were first mentioned in Figure 15.
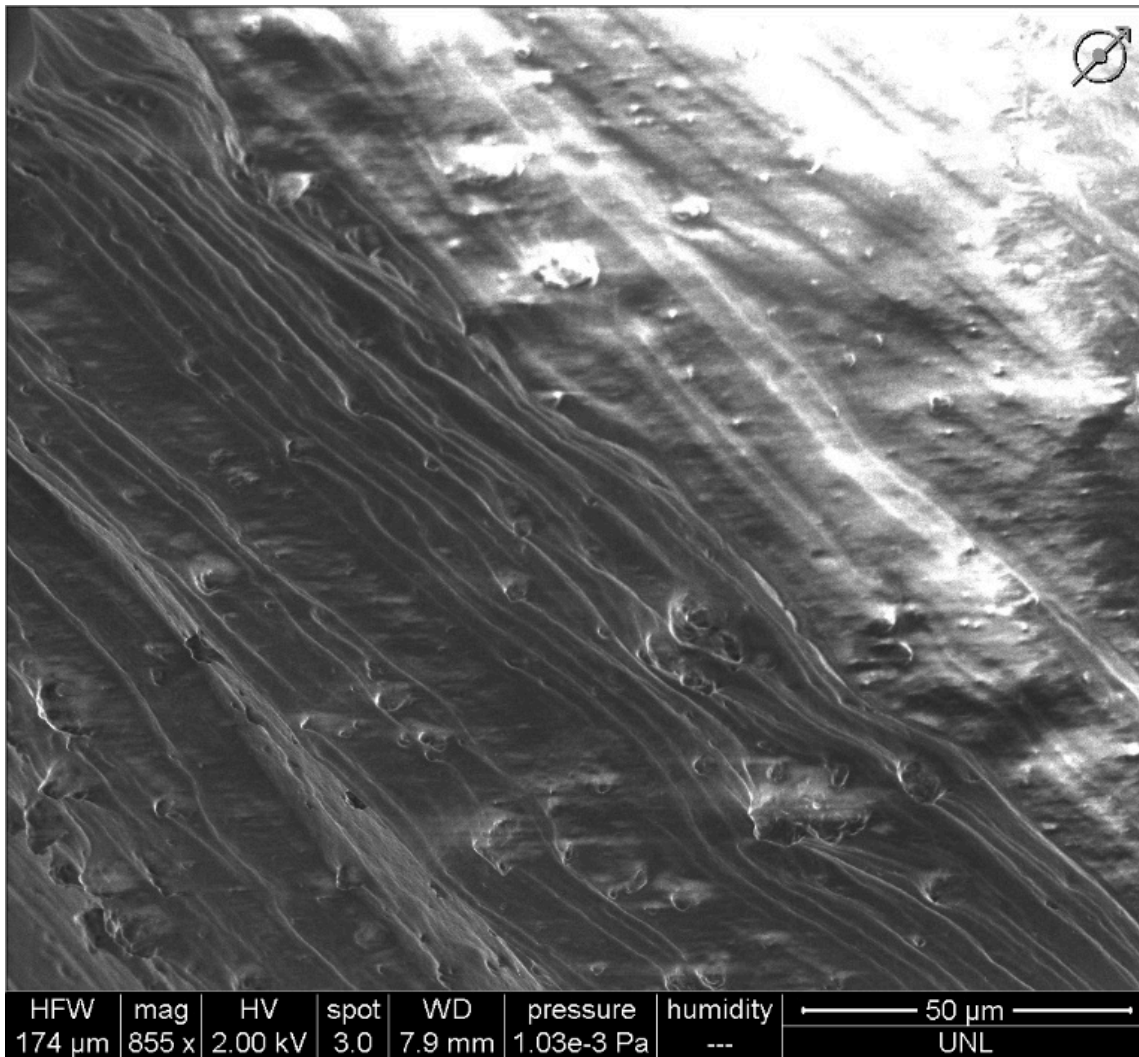
Fig. 17: SEM image of the pad printed using the silicon resin modified with 5% 1,6-bismaleimidohexane functionalized graphene powder viewed at 855x magnification. Morphology of the modified printed material has changed from non-fibrillar to fibrillar. The craters that were visible in Figure 15 on the base silicon print were not present on the sample modified with graphene.
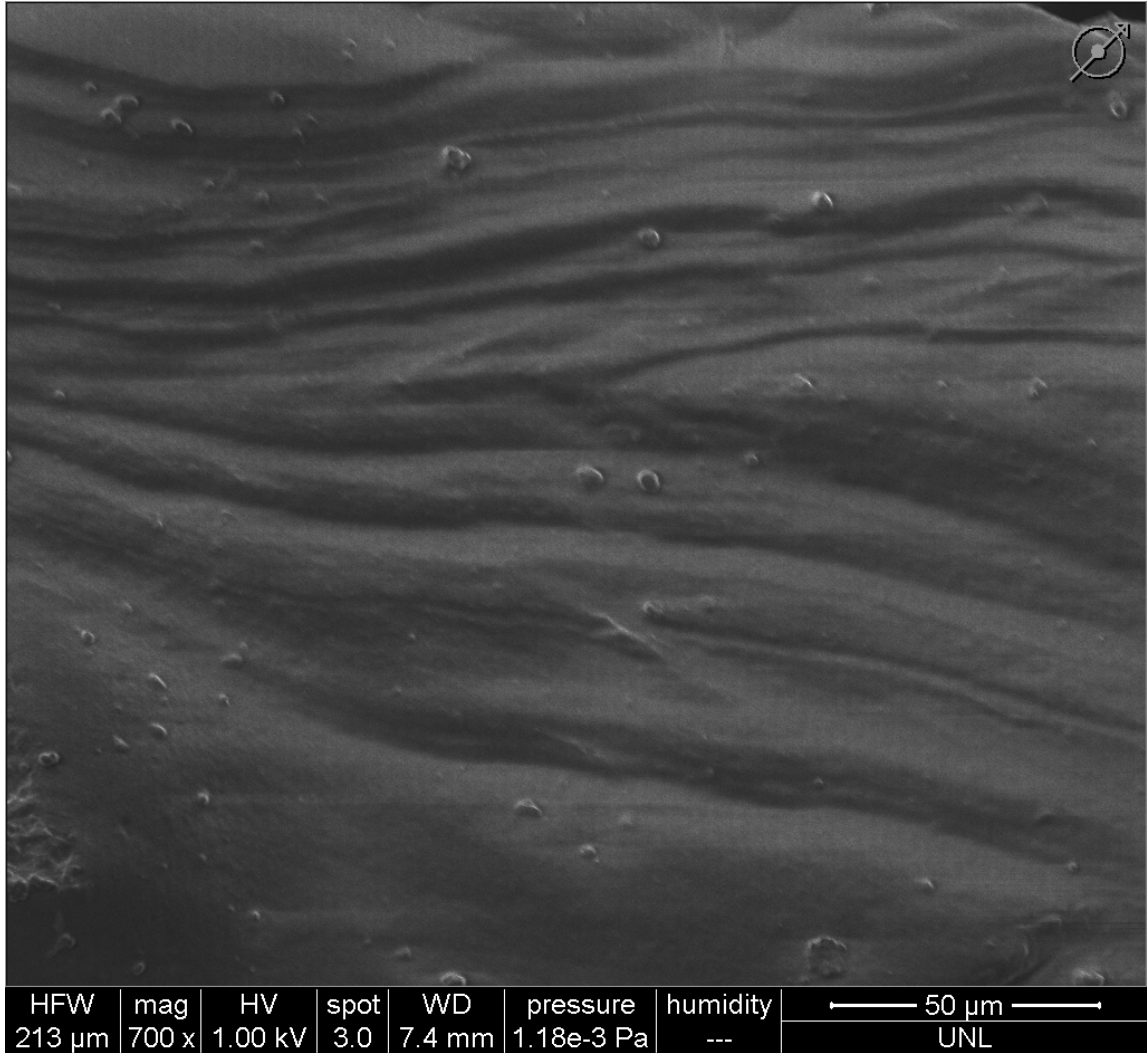
Fig. 18: SEM image of the pad printed using the silicon resin modified with 1.8% core-shell calcium carbonate/hydroxyapatite porous nanoparticles viewed at 700x magnification. Morphology altered similarly to how the graphene modified sample was altered. Surface morphology has converted from non-fibrillar to fibrillar. This modified sample does not have the craters on the surface that were present on the base silicone print.

Conclusions

With respect to the nanoindentation measurements, our modified material had no significant difference when compared to the original silicone material, which led us to a few conclusions. We have shown that there would not be a change in the hardness of the customized printed material at the concentrations we performed with graphene. However, given the strong mechanical properties graphene possesses, we hypothesized that a change in mechanical properties may still be possible, but that it would only occur at a concentration of graphene greater than 5% weight percent. The basis of this new hypothesis is focused on the fact that graphene largely gains its remarkable strength as a byproduct of the covalent bonding of graphene, which consists of 2D sheets of covalently bonded carbon atoms (Lee et al., 2008). Thus, it seems reasonable to hypothesize that a greater concentration of graphene powder may enable the resulting material to retain some of graphene's mechanical strength by allowing these sheets to form to a lesser extent within the mixture of silicone, or other materials. We were unable to test this hypothesis, as the 3D-Bioplotter encountered great difficulties when attempting to print silicone that included more than a weight percent of 5% of the 1,6-bismaleimidohexane functionalized graphene. Further research is necessary to answer the question of whether graphene holds promise as a viable additive capable of imbuing 3D printed objects with additional mechanical properties or strength.

When viewing the SEM images, it was interesting to see how the morphology of the printed material changed in both the graphene and calcium carbonate/hydroxyapatite samples. Looking at the unmodified silicone sample, there are visible craters within the surface. Craters of this size are incredibly worrisome when looking towards applications

of printed items. These craters are more than large enough to hold bacteria or physical buildup, thus creating a surface that will be harder to keep sanitary on a consistent basis. When looking at the graphene and the calcium carbonate/hydroxyapatite infused materials, neither displayed craters or divots. Instead, these materials had only dome shaped outcroppings, similar to what the base silicone sample displayed. It is worth noting that in comparison to the base silicone sample, the outcroppings found on both of the modified material samples are much smaller in size and are markedly less common in the calcium carbonate/hydroxyapatite sample specifically.   These outcroppings are much less hazardous with respect to the materials ability to be sanitized.

In addition to the conclusions stated previously there remain a few points to emphasize. First, we have shown that our specific modifications are possible with the equipment used. The 3D-Bioplotter is able to have additive modifications made to its existing printable materials and still successfully print with virtually no change to the specific print settings.   Functionalized graphene powder, specifically 1,6-bismaleimidohexane modified graphene powder can be added to acrylonitrile butadiene styrene beads at 0.64% weight percent to extrude a usable filament by the Filabot EX2. Similarly, this graphene powder could be added successfully at a weight percent of 1.2% to polycarbonate beads to produce a usable filament. This experiment displays some of the possible methods of modification available to customize existing 3D printer materials and displayed that this is an area where further exploration is possible.

CHAPTER 4

Discussion

A Look at Possible Applications

Our experiments made considerable headway in the field of augmenting current 3D printer materials, specifically with respect to graphene powder and calcium carbonate/hydroxyapatite nanoparticles. These materials, chosen primarily because of our group's familiarity working with both and our access to such materials, turned out to fit in well with the current landscape of research being conducted into 3D printing applications.

Graphene was chosen out of a desire to imbue existing 3D printer materials with more resistant nanoscale mechanical properties, and to include functional groups that could possibly have some drug delivery methodology. This belief was supported by research mentioned in the introduction, which has demonstrated that the loading of drugs or other compounds onto nanoparticles can allow for a controlled release in some situations, especially if there is a natural breakdown of the material over time.

The infusion of graphene into 3D printed materials with a biological or medical purpose, commonly referred to as bio printed materials, like the silicone used in the 3D-Bioplotter, could allow printing of individualized orthopedic devices that make use of the advantageous properties of graphene. In particular, materials modified via the incorporation of graphene have proven to be antimicrobial. This natural property of graphene to kill or stop the growth of microorganisms could work in tandem with a morphological change that may occur upon its incorporation into other materials. It could

be hypothesized that the inclusion of graphene into an otherwise cratered or generally uneven surfaced material could see the same benefits that the silicone material did in our studies. Those benefits being the virtual elimination of craters that microbes may be caught in during cleaning, and the creation of a fibrillar surface that could improve the cleanliness of any orthopedic device made with a graphene modified material.

In the near future, techniques like that used in Thangavel's lab to accelerate wound healing rates with graphene could be implemented with the specificity of 3D printing. The combination of these two technologies would allow medical professionals to construct a 3D printed bandage or dressing for the most painful of wounds. This would allow medical staff to maximize the comfort levels for those needing individualized wound dressings through the use of precise 3D printers able to perfectly match the size, shape and depth of a wound after scanning the injury. The future of this technology could allow for the printing of wound dressings with a patient specific, functional design that could also ensure a shorter and more effective healing process.

Given that the antibacterial properties of the calcium carbonate and hydroxyapatite nanoparticles already documented in vitro, the safe insertion and use of such materials in vivo has become the next major goal. The work of the Jiangsu group may one day be combined with the customizability of 3D printing to allow a patient specific 3D printed biological tissue to be injected with their gel scaffold. Theoretically, this 3D printed item could then be implanted into a patient and allow for bone regeneration using the 3D printed tissue as a bone deposition blueprint for the body to integrate with. Bone repair of this sort would revolutionize bone treatment, benefitting sufferers of bone injury and bone defects alike.

In conclusion, our research conducted in conjunction with UNL and the NNF may seem limited in scope, yet the applications available when combining our materials, techniques, and findings with pertinent research in the fields of biology and medicine holds a great deal of promise. The application of customized 3D printed materials in a healthcare setting used to be something one would only dare speculate about just a couple years ago. As we continue to find success interfacing the technology of 3D printers with cutting edge research, these speculations become increasingly realistic. While the actual widespread implementation of the applications discussed above are far from being fully realized, it is reasonable to say researchers in this field are innovating at a remarkable rate. There is a lot of work to be done regarding any one of these future applications, yet the knowledge that there exists a framework for engineering such futuristic applications is promising and ensures similar research will continue towards improving patient care and individual outcomes for many years to come.

REFERENCES

3D Printing for Beginners. (n.d.). *3D Printing Technology*. Retrieved from
    http://3dprintingforbeginners.com/wp-content/uploads/2014/04/3D-Printing-
    Technology_Download.pdf

American Society of Mechanical Engineers. (2016, May 18). 3D Systems' First 3D Printer
    named Historic Mechanical Engineering Landmark by ASME. Retrieved from
    https://www.asme.org/about-asme/media-inquiries/press-releases/3d-systems-
    first-3d-printer-named-historic-mechani

AMFG. (2020, January 27). 3D Printing with Polymers: All You Need to Know. Retrieved
    from https://amfg.ai/2019/01/17/3d-printing-with-polymers-all-you-need-to-
    know/

Bourell, D. L., Beaman, J. J., Leu, M. C., & Rosen, D. W. (2009). A Brief History of Additive
    Manufacturing and the 2009 Roadmap for Additive Manufacturing: Looking Back
    and Looking Ahead. *Proceedings of RapidTech 2009: US-TURKEY Workshop on
    RapidTechnologies*. Retrieved from
    https://pdfs.semanticscholar.org/4716/c69f0b90a158589e54248a524a57ad78f4
    a3.pdf

Grant, T. (2005). *International Directory of Company Histories* (Vol. 67). Amsterdam,
    Netherlands: Amsterdam University Press.

Kodama, H. (1981). Automatic method for fabricating a three-dimensional plastic model
    with photo-hardening polymer. *Review of Scientific Instruments*, *52*(11), 1770–
    1773. https://doi.org/10.1063/1.1136492

Lee, C., Wei, X., Kysar, J. W., & Hone, J. (2008). Measurement of the Elastic Properties
    and Intrinsic Strength of Monolayer Graphene. *Science*, *321*(5887), 385–388.
    https://doi.org/10.1126/science.1157996

Mohd Abd Ghafar, S. L., Hussein, M. Z., Rukayadi, Y., & Abu Bakar Zakaria, M. Z. (2017).
    Surface-functionalized cockle shell–based calcium carbonate aragonite
    polymorph as a drug nanocarrier. *Nanotechnology, Science and Applications*,
    Volume 10, 79–94. https://doi.org/10.2147/nsa.s120868

Pîrjan, A., & Petrosanu, D. (2013). THE IMPACT OF 3D PRINTING TECHNOLOGY ON THE
    SOCIETY AND ECONOMY. *Journal of Information Systems & Operations
    Management*, 1–11. Retrieved from https://search-proquest-
    com.ezproxy.usd.edu/docview/1477205392?accountid=14750

PubChem. (2020a, March 28). 1,6-Bismaleimidohexane. Retrieved from
https://pubchem.ncbi.nlm.nih.gov/compound/1_6-Bismaleimidohexane

PubChem. (2020b, April 6). N-Hexadecylmaleimide. Retrieved from
https://pubchem.ncbi.nlm.nih.gov/compound/4526314#section=2D-Structure

Ren, B., Chen, X., Du, S., Ma, Y., Chen, H., Yuan, G., … Niu, X. (2018). Injectable
polysaccharide hydrogel embedded with hydroxyapatite and calcium carbonate
for drug delivery and bone tissue engineering. *International Journal of Biological
Macromolecules*, *118*, 1257–1266.
https://doi.org/10.1016/j.ijbiomac.2018.06.200

Rodriguez, R. X. (2014). *Characterization of direct print additive manufacturing process
for 3D build of a carbon nanostructure composite* (Master's thesis). Retrieved
from https://search-proquest-
com.ezproxy.usd.edu/docview/1615403043?accountid=14750

Sereda, G., & Keppen, J. (2015). *U.S. Patent No. 10316010*. Washington, DC: U.S. Patent
and Tradmark Office.

Stratasys Direct Manufacturing. (2017, August 30). Key Considerations when 3D Printing
with Thermoplastics. Retrieved from
https://www.stratasysdirect.com/materials/thermoplastics/3d-printing-
thermoplastics-key-considerations

Tegou, E., Magana, M., Katsogridaki, A., Ioannidis, A., Raptis, V., Jordan, S., … Tegos, G.
P. (2016). Terms of endearment: Bacteria meet graphene nanosurfaces.
Biomaterials, *89*, 38–55. https://doi.org/10.1016/j.biomaterials.2016.02.030

Thangavel, P., Kannan, R., Ramachandran, B., Moorthy, G., Suguna, L., & Muthuvijayan,
V. (2018). Development of reduced graphene oxide (rGO)-isabgol nanocomposite
dressings for enhanced vascularization and accelerated wound healing in normal
and diabetic rats. *Journal of Colloid and Interface Science*, *517*, 251–264.
https://doi.org/10.1016/j.jcis.2018.01.110

Wohlers, T., & Gornet, T. (2016). *Wohlers Report 2016: History of Additive
Manufacturing*. Retrieved from
https://www.wohlersassociates.com/history2016.pdf